LBL-14352
Preprint

Lawrence Berkeley Laboratory
UNIVERSITY OF CALIFORNIA

ENERGY & ENVIRONMENT
DIVISION

To be submitted to the International Journal of
Heat and Mass Transfer

NATURAL CONVECTION IN SHALLOW ENCLOSURES WITH DIFFERENTIALLY HEATED END WALLS AND NONADIABATIC HORIZONTAL WALLS

A. Gadgil and G. Shiralkar

May 1983

ENERGY AND ENVIRONMENT DIVISION

Prepared for the U.S. Department of Energy under Contract DE-AC03-76SF00098

LBL-14352
31 May 1983

NATURAL CONVECTION IN SHALLOW ENCLOSURES WITH DIFFERENTIALLY HEATED END WALLS AND NONADIABATIC HORIZONTAL WALLS*

Ashok Gadgil
Passive Research and Development Group
Lawrence Berkeley Laboratory
University of California
Berkeley, California 94720

and

Gautam Shiralkar#
Mechanical Engineering Department
University of California
Berkeley, California 94720

ABSTRACT

Numerical studies of laminar natural convection at high Ra numbers in shallow enclosures are reported. In these studies the working fluid is allowed to interact with the horizontal walls. It is shown that even a small amount of heat loss from these walls can lead to a flow structure qualitatively different from the more commonly studied situation where the horizontal walls are adiabatic. This is particularly important in applications where the mass transfer and flow structure are of interest. The results highlight the difficulty in practice of both approximating the adiabatic horizontal wall condition, and interpreting experimental data.

INTRODUCTION

Previous work on steady laminar natural convection in shallow enclosures has concentrated on flows bounded by adiabatic horizontal walls [1,2]. In practice, however, it is difficult to obtain ideal

---

*This work was supported by the Assistant Secretary for Conservation and Renewable Energy, Office of Solar Heat Technologies, Passive and Hybrid Solar Energy Division, of the U.S. Department of Energy under Contract No. DE-AC03-76SF00098.

#Gautam Shiralkar was a graduate student at the University of California, Berkeley, at the time this research was done and is presently employed at Sohio Petroleum Company, San Francisco, CA 94111.

insulation conditions, and some heat transfer to the horizontal walls will generally occur. When the horizontal walls are adiabatic, their surface temperature is determined by the convection process (in the absence of radiation). If the horizontal walls are made from highly conducting material, or if the end walls have high radiant emissivity, the surface temperature along the horizontal walls is a linear function of distance. Such thermal boundary conditions are encountered in the slots of superconducting rotating electric machines [3], and also in solar flat-plate collectors having rectangular honeycombs for suppression of convective heat losses [4]. If the horizontal walls are constructed of a material that cannot be approximated by either a perfect conductor or a perfect insulator, and some thermal interaction with the external environment will occur. This is a common situation; for example, the circulation in the Red Sea and thermal flows in estuaries have been analyzed by comparing them with convection in shallow horizontal enclosures [5,6,7]. Some thermal interaction at the (upper) horizontal surfaces of the fluid would be likely to occur in both these cases. Crystal growth [1,8] is another situation in which the horizontal walls of the apparatus cannot be considered adiabatic. As a final example, the thermal boundary conditions considered in this paper are important in the study of convective heat transfer in a plenum space shared by two building zones at different temperatures.

Most laboratory tests with shallow enclosure convection bounded by insulated horizontal walls also involve some heat transfer across the horizontal walls. The purpose of the study reported here is to examine the effect of this heat transfer on the convection process in the enclosure. The end walls of the shallow enclosure [$A = O(0.1)$] are assumed to be isothermal and at different temperatures; two kinds of thermal boundary conditions for the horizontal walls have been examined:

- Case I: Horizontal walls having a linear temperature profile (Fig. 1a).
- Case II: Horizontal walls allowing thermal interaction with the external environment specified by a heat transfer coefficient (Fig. 1b).

Case I has been studied analytically in the limit of low Ra (or low A), and has been studied numerically at high Ra values ($Ra \leq 10^9$). Case II has been numerically studied at a high Ra number ($Ra = 3\times10^8$) for various values of heat transfer coefficients. Significant qualitative differences are found in the temperature and flow fields under these conditions when compared to the flow bounded by adiabatic horizontal walls. Correlations for heat transfer rates for both horizontal and vertical walls are presented for Case I.

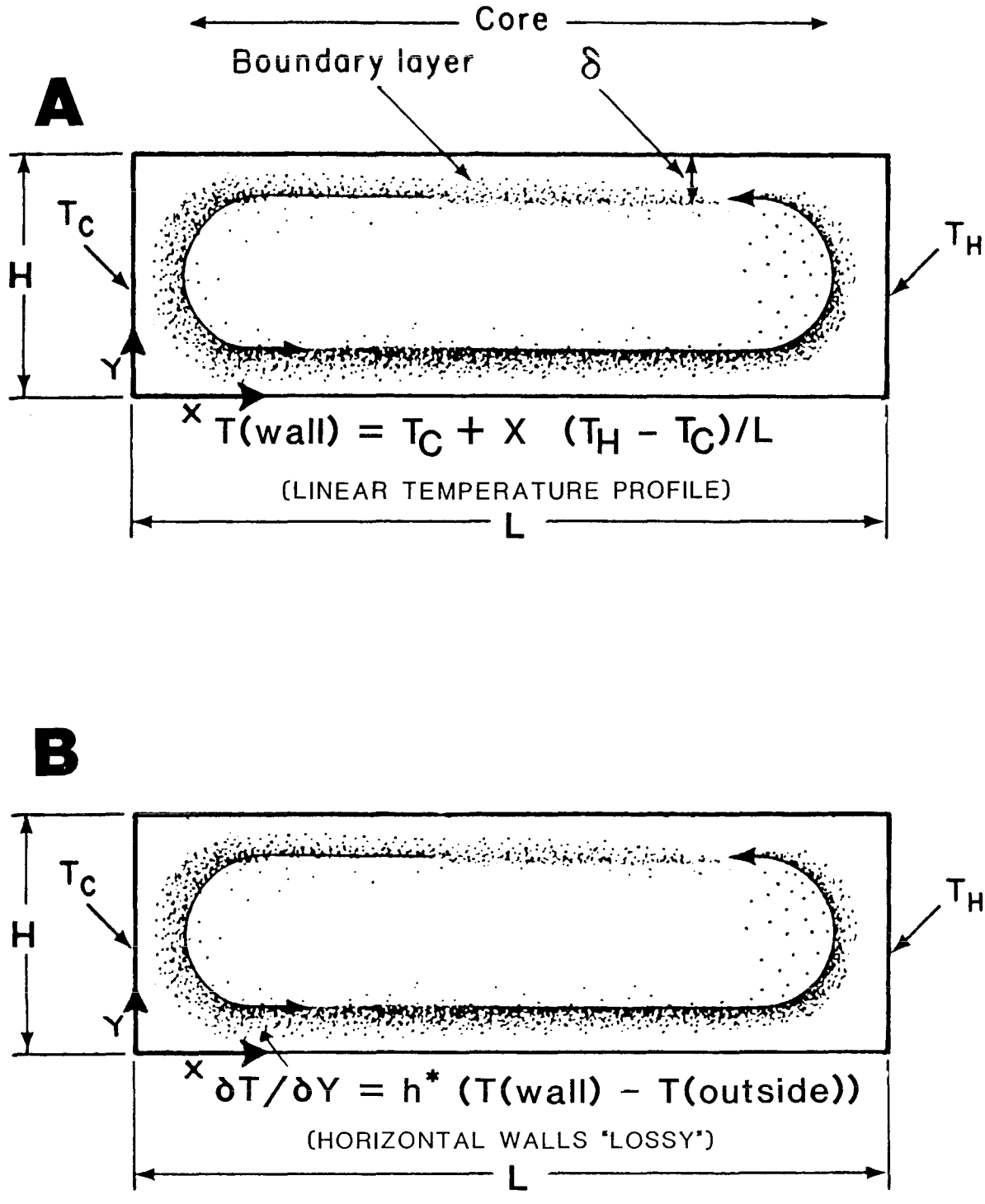

XBL 836-10129

Figures 1a,b. Schematics of Enclosure Geometry

GOVERNING EQUATIONS AND NUMERICAL PROCEDURE

The two-dimensional rectangular enclosure (Figs. 1a and 1b) contains a Boussinesq fluid of unit Prandtl number. The governing steady-state equations are:

Continuity:
$$\vec{\nabla} \cdot \vec{V} = 0 \tag{1}$$

Momentum:
$$(\vec{V} \cdot \vec{\nabla})\vec{V} = \nabla^2 \vec{V} - \vec{\nabla} p + Gr\theta \hat{j} \tag{2}$$

Energy:
$$(\vec{V} \cdot \vec{\nabla})\theta = \left(\frac{1}{Pr}\right)\nabla^2 \theta \tag{3}$$

where $\vec{V}$ and θ denote velocity and temperature, nondimensionalized, using scales ΔT, ν, and H, for the temperature, kinematic viscosity, and length respectively.

The thermal boundary conditions for the vertical (end)walls are:

$$\begin{aligned} X = 0 \quad &\Rightarrow \quad \theta = -0.5 \\ X = \frac{1}{A} \quad &\Rightarrow \quad \theta = 0.5 \quad . \end{aligned} \tag{4a}$$

For the horizontal walls two sets of boundary conditions have been examined. They are (1) linear temperature profile:

$$\left.\begin{aligned} Y &= 0 \\ Y &= 1 \end{aligned}\right\} \quad \Rightarrow \quad \theta = (AX - 0.5) \tag{4b}$$

or (2) a specified interaction with the environment:

$$\begin{aligned} Y = 0 \quad &\Rightarrow \quad \frac{d\theta}{d\theta} = h(\theta - \theta_{env}) \\ Y = 1 \quad &\Rightarrow \quad \frac{d\theta}{d\theta} = h(\theta_{env} - \theta) \quad . \end{aligned} \tag{4c}$$

Numerical solutions to Eqs. (1-4) were obtained at low Ra numbers (Ra = $O(10^3)$) using the finite difference code, FIRE1, described in [9]. The simulations used the vorticity-stream function formulation on an evenly spaced 17 X 41 grid at an aspect ratio of 0.1.

Numerical solutions at high Ra numbers ($10^6 \leq Ra \leq 3 \times 10^9$) were obtained using a finite difference code based on the Patankar-Spalding finite difference scheme, described in detail in [10]. Predictions from this code for high Ra convection in enclosures have yielded good agreement with experiment and analysis [11, 12, 13]. These simulations used a variable-spaced grid of 31 X 37 nodes with

a high density of grid lines near the solid boundaries, and relatively sparse spacing away from the walls. The smallest grid spacing (dimensionless) was 0.002, resulting in excellent resolution of the boundary layers on all the solid boundaries. Typically each simulation required 700 seconds of execution time on a CDC 7600 installation, and the simulations were terminated when the field residues were less than 10^{-5}.

HORIZONTAL WALLS WITH A LINEAR TEMPERATURE PROFILE (CASE I)

Experimental investigations of fluid flow in shallow enclosures with experimental boundary conditions approximating Case I have been reported by Ostrach, et al. [8], and by Boyak and Kearney [14]. Numerical studies have been reported by Cormack, et al. [15,16], by Wirtz and Tseng [17], and Klosse and Ullersma [18] at moderate values of Ra. The present work uses analytic techniques [9] to examine the low Rayleigh number regime, in the limit $Ra \to 0$. At high Rayleigh numbers, boundary layers are formed lining both the vertical and horizontal walls; in some cases this flow changes from the usual unicellular structure to a tricellular structure. In this region, numerical techniques have been used to study the flow. In order to check the consistency of the analytic and numerical techniques, comparisons have been made between their predictions at small Rayleigh numbers.

Low A or Low Ra Regime (Case I)

For very shallow enclosures in the limit $A \to 0$, or alternatively with $Ra \to 0$, the flow will be similar to that studied by Cormack, et al., [15, 16], and by Imberger [7], who found that the temperature was distributed linearly along the adiabatic horizontal walls. The flow in the core (i.e., away from the end walls) of the enclosure under these conditions will be a parallel counterflow, with the end walls acting chiefly to turn the flow around.

The following asymptotic expansion is made in powers of the aspect ratio, A, for the flow in the core:

$$\begin{aligned} U(X,Y) &= U_0(X,Y) + AU_1(X,Y) + A^2U_2(X,Y) + \ldots \\ V(X,Y) &= V_0(X,Y) + AV_1(X,Y) + A^2V_2(X,Y) + \ldots \\ \theta(X,Y) &= \theta_0(X,Y) + A\theta_1(X,Y) + A^2\theta_2(X,Y) + \ldots \end{aligned} \tag{5}$$

Using this expansion, a solution is obtained to Eqs. (1-4)

which is valid for all powers of A:

$$U(X,Y) = (1/12)\ A\ Ra\ Y\ (2Y-1)\ (Y-1) \tag{6a}$$

$$V(X,Y) = 0 \tag{6b}$$

$$\theta(X,Y) = \bar{X} + (1/720)\ A\ Ra\ Y\ (Y-1)\ (2Y-1)\ (3Y^2-3Y-1) \tag{6c}$$

where

$$\bar{X} = A\ X - 0.5 \quad .$$

The flow profile (Eqs. 6a and 6b) is found to be identical to that obtained in [16] for the case of adiabatic walls, but the temperature profile, Eq. (6c), is different because it allows for heat exchange with the horizontal walls. The Nusselt number for vertical heat transfer, Nu_v, (i.e., the average Nusselt number in the core on the horizontal walls) can now be determined:

$$Nu_v = A\int_0^{1/A} -\frac{\partial\theta}{\partial Y}\bigg|_{Y=0} dx = A\int_0^{1/A} \frac{\partial\theta}{\partial Y}\bigg|_{Y=1} dx = \left(\frac{1}{720}\right) A\ Ra^2 \quad . \tag{7}$$

The Nusselt number, Nu_h, for horizontal heat transfer is:

$$Nu_h = \int_0^1 \left(U\theta - \frac{\partial\theta}{\partial X}\right) dY = \frac{1}{1209600} A^3Ra^2 + A \quad . \tag{8}$$

This is considerably smaller than the Nusselt number for the adiabatic horizontal walls case, which is [19]:

$$Nu_h^* = \frac{1}{362880} A^3Ra^2 + A \quad .$$

Equations (6a-c) can also be derived for $Ra \to 0$ by formulating the asymptotic expansion in powers of Ra.

The temperature profile from Eq. (6c) is compared with a numerically obtained temperature profile in Fig. 2a; the velocity profile, Eq. (6a), is compared in Fig. 2b. The comparisons are shown for flow at $Ra = 10^3$, $A = 0.1$, and $Pr = 1.0$. The agreement is very good.

High Ra Regime (Case I)

If the enclosure is shallow enough, viscous effects will produce a fully developed, inertia-free, S-shaped velocity profile

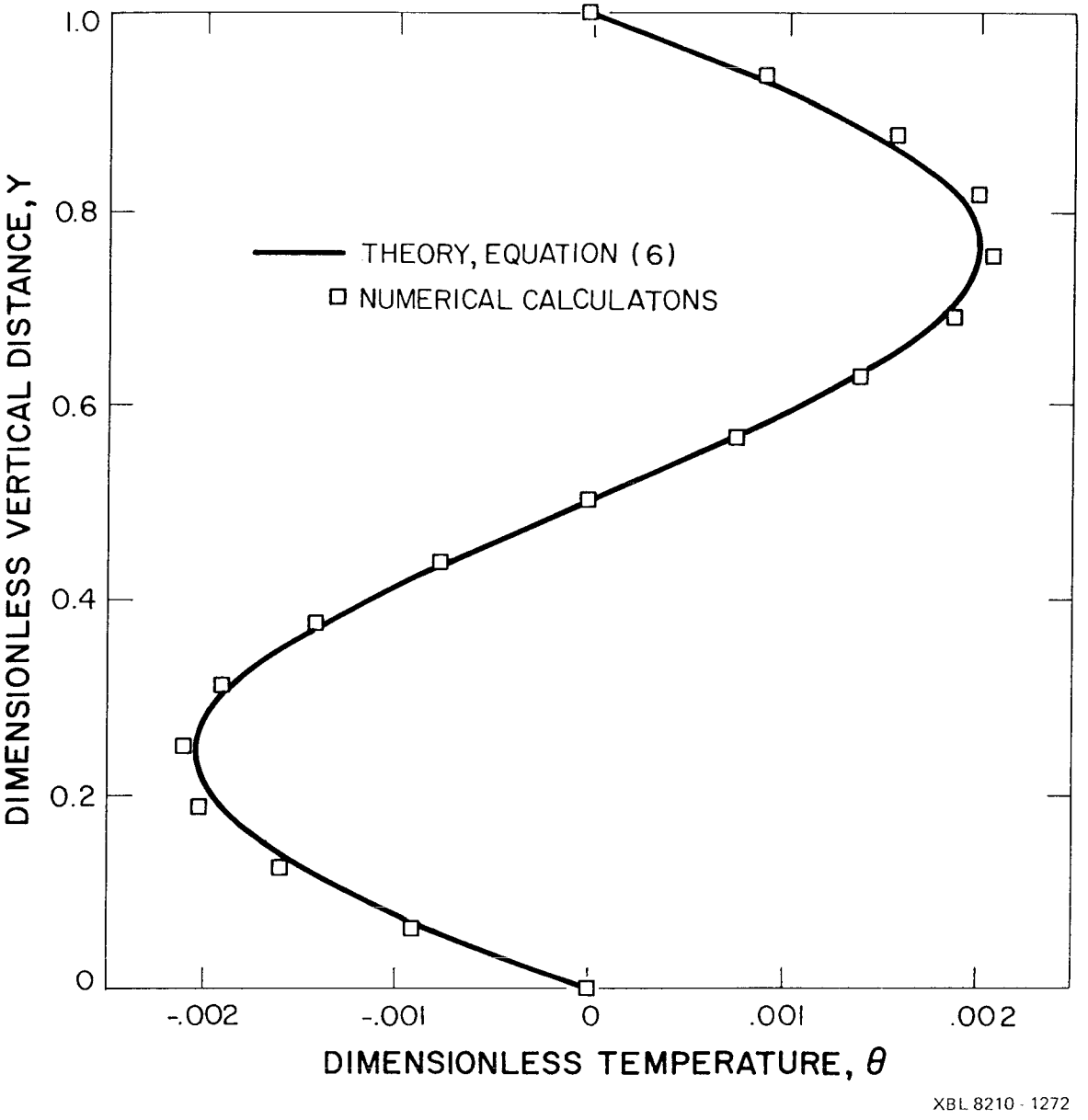

Figure 2a. Low Ra Temperature Profile at Midsection (Case I)

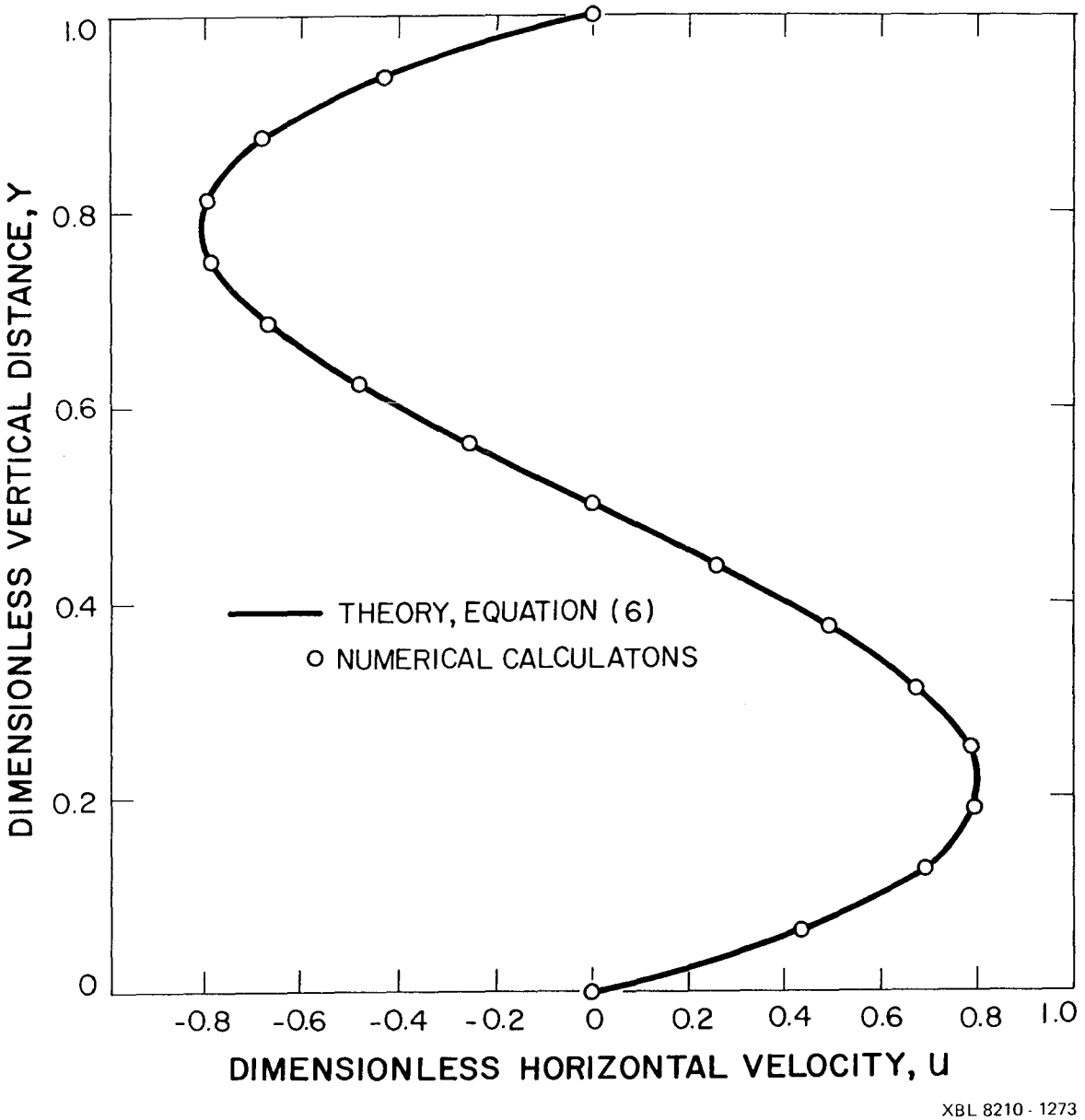

Figure 2b. Low Ra Velocity Profile at Midsection (Case I)

[Eqs. (6a, b)] in the core. As Ra is increased to high enough values, boundary layers will appear on the horizontal walls as well, persisting throughout the core region of the enclosure. This is similar to the situation studied earlier for adiabatic walls [12, 19]; there are, however, significant qualitative differences, particularly in the flow structure. Specifically, at high values of Ra, flow reversal can occur in the center of the enclosure. This has not been previously predicted numerically -- probably because numerical investigations at such high values of Ra have only recently become possible -- but has been demonstrated in experiments in which the thermal boundary conditions on the horizontal walls were not perfectly adiabatic (e.g., [20]). This flow reversal is caused by the heat transfer at the horizontal walls. For the same aspect ratio and Rayleigh number, Case I is found to have a lower thermal stratification in the midcore, and substantially higher velocities than the adiabatic walls case. In fact, the peak horizontal velocity in the core was found to differ by about a factor of two between the two cases.

Numerically predicted velocity profiles in the enclosure center are presented for $A = 0.2$, $Ra = 10^7$, 10^8, and 10^9 in Fig. 3. For comparison, a velocity profile for flow at $Ra = 10^8$ bounded by adiabatic horizontal walls is also shown. The boundary layer structure is evident. The horizontal boundary layers in Case I have a substantially larger amount of buoyancy ($Ra\ \partial\theta/\partial X = Ra\ A$) driving them than the adiabatic walls case where ($\partial\theta/\partial X$) is almost equal to zero in the core. In the situation where the walls are adiabatic, the velocities near the midheight of the core are not very small, and inertia effects are important almost all the way to the center. In the present case, the velocities are attenuated much faster as one moves towards the midheight. As Ra is increased still further, a flow reversal occurs in the enclosure.

The corresponding temperature profiles at $Ra = 10^8$ are shown in Fig. 4, together with the temperature profile for flow with adiabatic horizontal walls. The Case I temperature profiles show a smaller degree of stratification in the core. Owing to heat transfer at the horizontal boundaries, a strong temperature inversion arises in the boundary layers near the horizontal walls. As the Rayleigh number is increased for a fixed aspect ratio, flow velocities in the horizontal boundary layers increase, and the temperature inversion becomes more pronounced. On the other hand, as the aspect ratio is decreased for a fixed value of Ra, the temperature gradient along the horizontal walls decreases and the temperature inversion becomes less pronounced. This temperature inversion is responsible for the change in the flow pattern.

The temperature inversion at the horizontal walls is "convected" into the vertical boundary layer before its dissipation by diffusion in the core. This results in a very strong temperature inversion at each of the vertical walls (Fig. 5a), and produces a

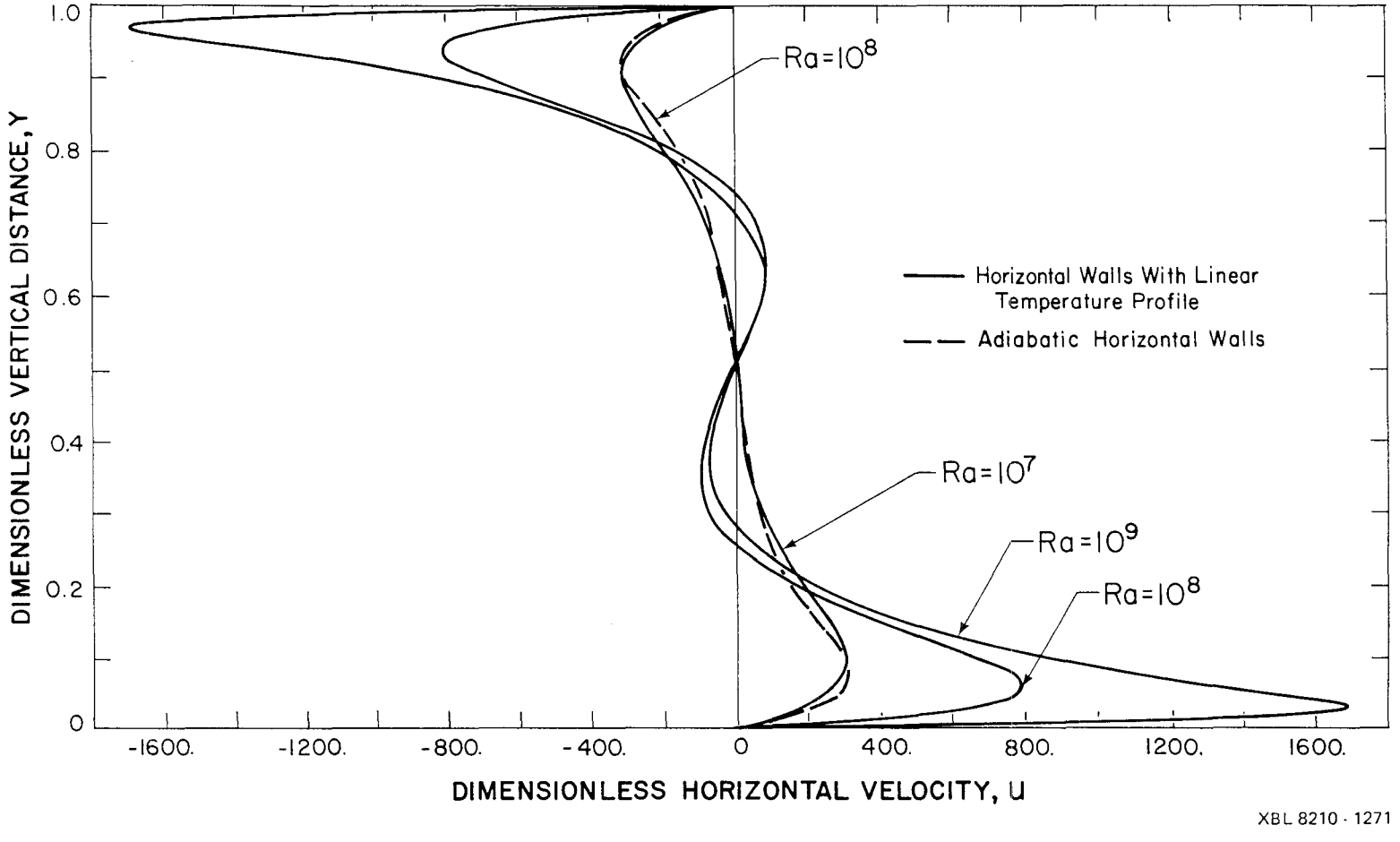

Figure 3. High Ra Velocity Profiles at Midsection (Case I)

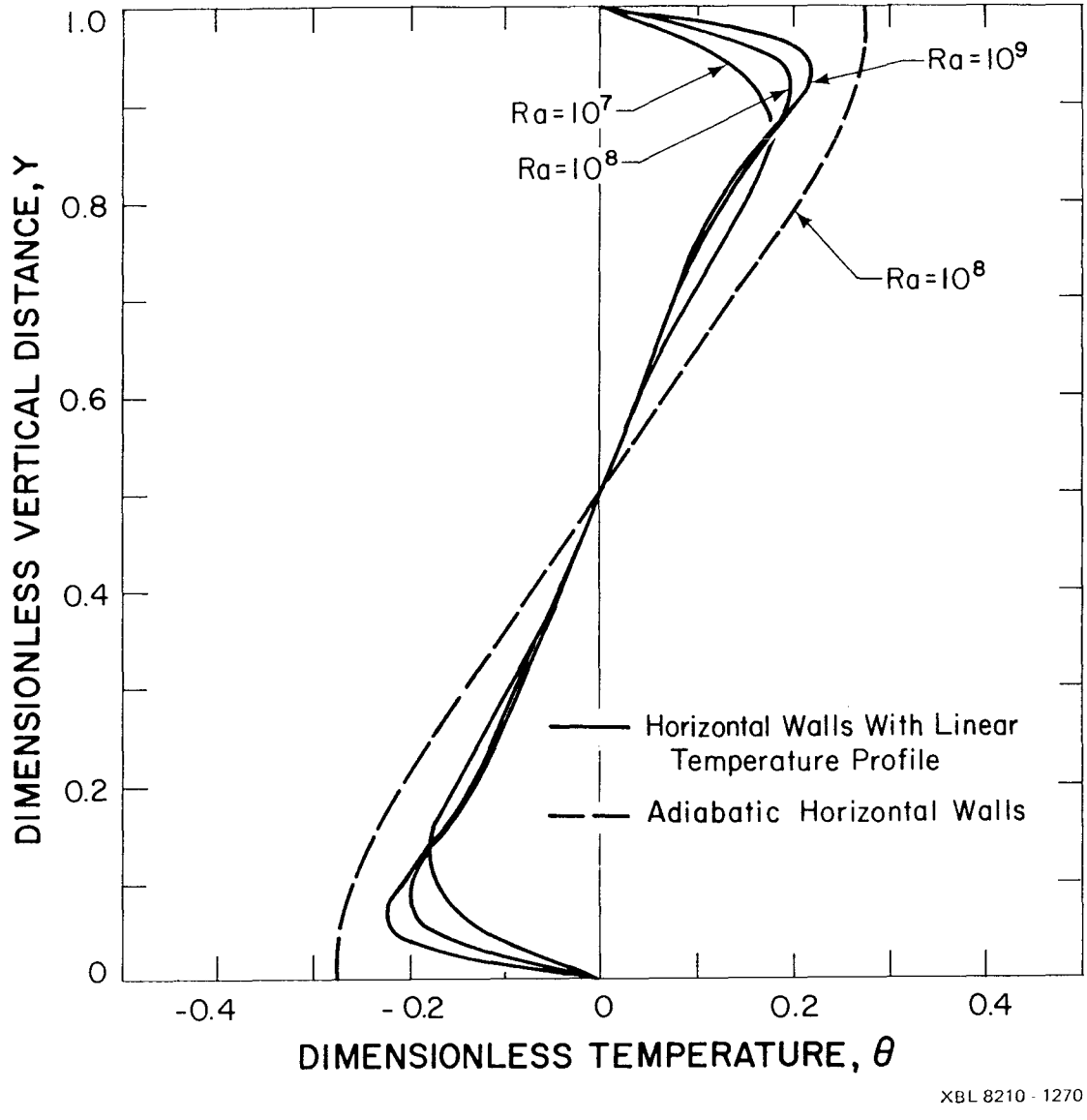

Figure 4. High Ra Temperature Profiles at Midsection (Case I)

strong opposite vorticity within the vertical boundary layer, thereby causing the vertical flow to reverse (Fig. 5b). In a study of convection in shallow enclosures at a much lower Ra number, Ra = 1.25×10^5, Wirtz and Tseng [17] also report a small flow reversal at the end walls. At that value of Ra, there was no flow reversal in the core and the tricellular structure of Fig. 6a was not observed. The present simulations indicate that at A = 0.2, the flow reversal occurs in the core only at Ra values exceeding 3×10^7. (For adiabatic walls, too, a temperature inversion in the vertical boundary layers is produced, but this inversion is not as strong as that caused by the heat transfer to the horizontal walls, and does not cause flow reversal in the core.) This reversed flow from the outer edge of the vertical boundary layer continues back into the core of the enclosure, where it loses its momentum and becomes entrained into the approaching horizontal wall boundary layer flow. Streamlines for this flow are shown in Fig. 6a. The corresponding isotherms are shown in Fig. 6b.

Al-Homoud and Bejan [20] experimentally investigated natural convection in a shallow enclosure with A = 0.0625, Pr = 6.3, for $2 \times 10^8 \leq Ra \leq 2 \times 10^9$. They showed velocity boundary layers in the core on the horizontal walls getting rapidly attenuated towards the midheight and reversing direction in the core (see their Fig. D2). The authors report that heat transfer did occur at both horizontal walls, the net heat loss from their apparatus to the ambient air being about 12 percent. This experiment provides strong support for our numerical predictions of a qualitatively new core flow structure under conditions of heat transfer to the horizontal boundaries.

In the boundary layer, the following equations may be written using standard boundary layer approximation. The length scale in the x direction is

$$x = O\left(\frac{1}{A}\right)$$

and in the y direction is

$$y = O(\delta) \quad ,$$

where δ is the thickness of the horizontal boundary layer in the core. The scale for U is set equal to Γ. Then from Eq. (1) one can write $V = O(\Gamma\delta A)$, and from Eq. (3) $A = O(1/\delta^2)$. Using these relations in Eq. (2) with $\theta = O(1)$ and Pr = O(1), one gets

$$\frac{A\Gamma^2}{\delta} = O(RaA) \quad .$$

Solving for Γ and δ one obtains:

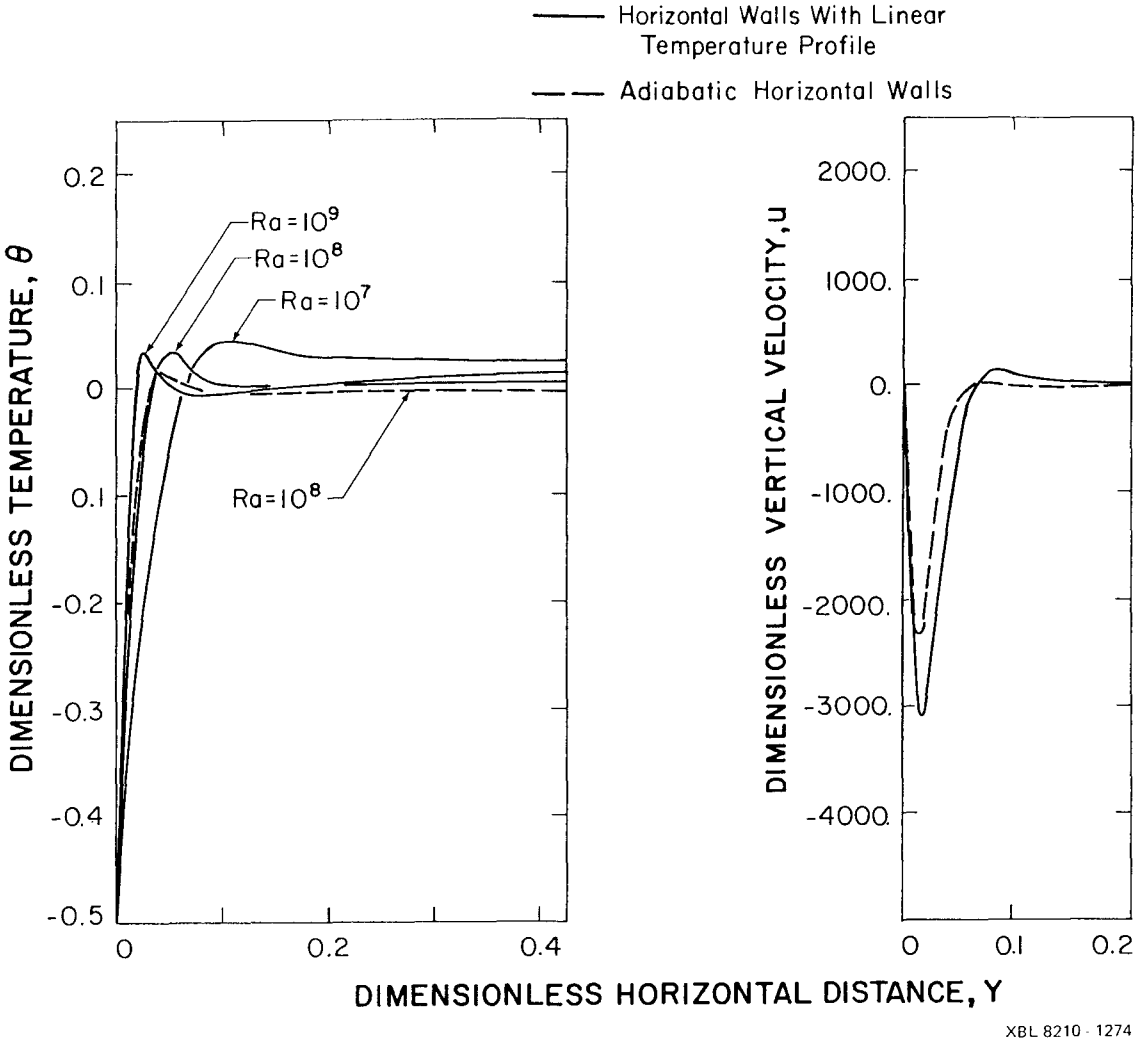

Figures 5a,b. Temperature and Velocity Profiles Near the Cold Vertical Wall (Case I)

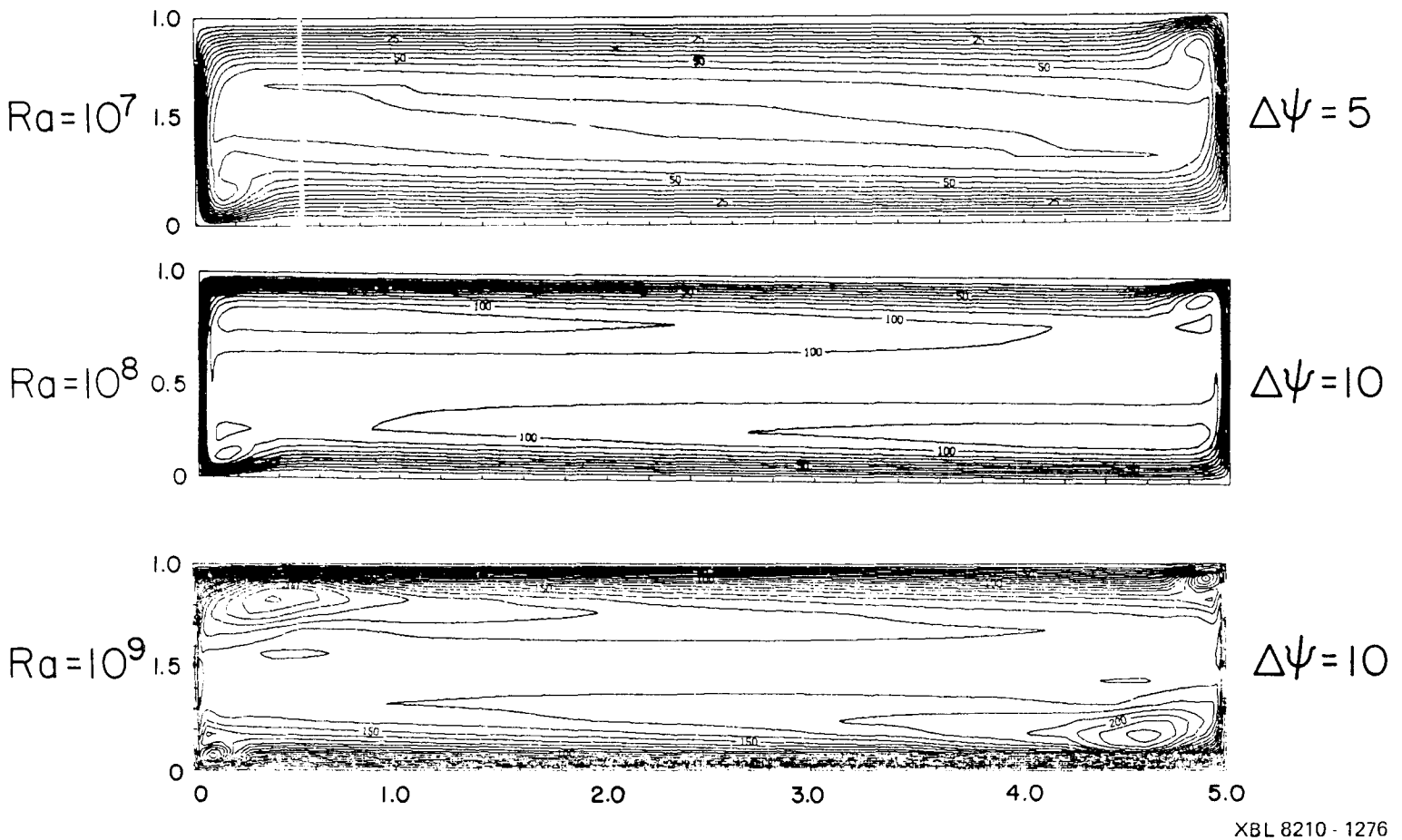

Figure 6a. Streamlines for Case I (note tricellular structure at high Ra)

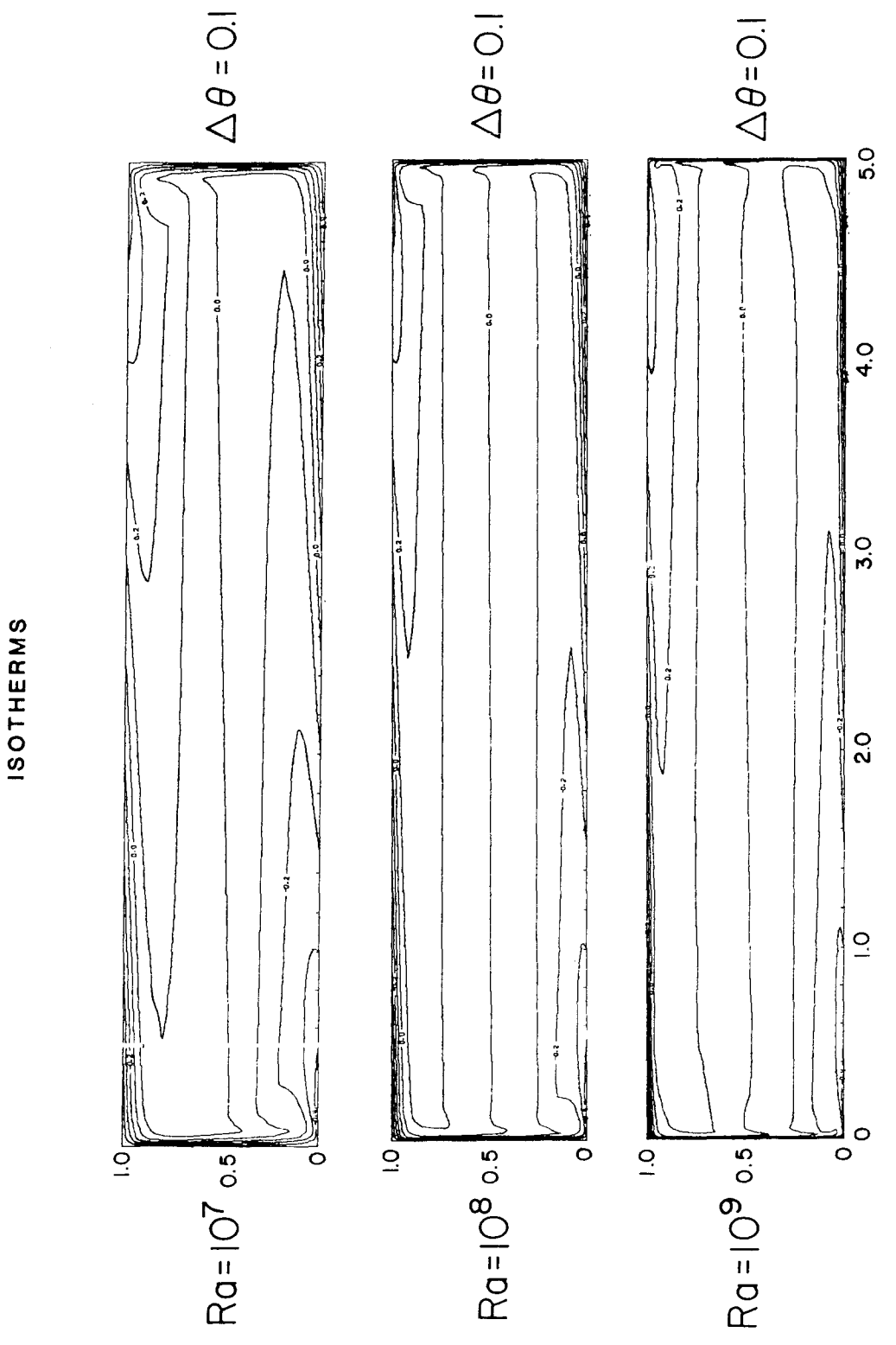

Figure 6b. Isotherms for Case I

$$\Gamma = O(Ra^{0.4}A^{-0.2})$$

and

$$\delta = O(Ra^{-0.2}A^{-0.4}) \quad .$$

The heat loss from the horizontal wall can be estimated as

$$Nu_v = O\left(\frac{1}{\delta}\right) = O(Ra^{0.2}A^{0.4}) \quad . \tag{9}$$

The Nusselt number on the horizontal walls, obtained from the numerical simulations, is shown plotted as a function of Ra for two values of A in Fig. 7, and fits the following single equation:

$$Nu_v = 0.134\ Ra^{0.23}A^{0.5} \quad . \tag{10}$$

The calculated values of Nu_h are plotted against Rayleigh numbers in Fig. 8. The log Nu-log Ra curves show a continuous decrease in slope, with the slope tending to 0.25 at high values of Rayleigh number. This is similar to the situation where the horizontal walls are adiabatic, where the change in slope to an asymptotic value of 0.25 arises from the increasing independence of the vertical wall boundary layers from the core [12]. The Nusselt numbers of Case I are lower than those of the case of adiabatic walls mainly due to the preheating and precooling of the fluid as it approaches the hot and cold end walls. Smart, et al., [4] experimentally, and Wirtz and Tseng [17] numerically, have also demonstrated this effect at lower Ra.

The heat transfer results, Fig. 8, from the present simulations were correlated as follows:

$$Nu_h = (2^{-3/2})\ Ra^p \tag{11}$$

where

$$A = 0.1 \Rightarrow p = 0.25 - .53\ Ra^{-.1385} \tag{12}$$

and

$$A = 0.2 \Rightarrow p = 0.25 - .484\ Ra^{-.1450} \quad . \tag{13}$$

Equations (11-13) fit all the data to within 5 percent.

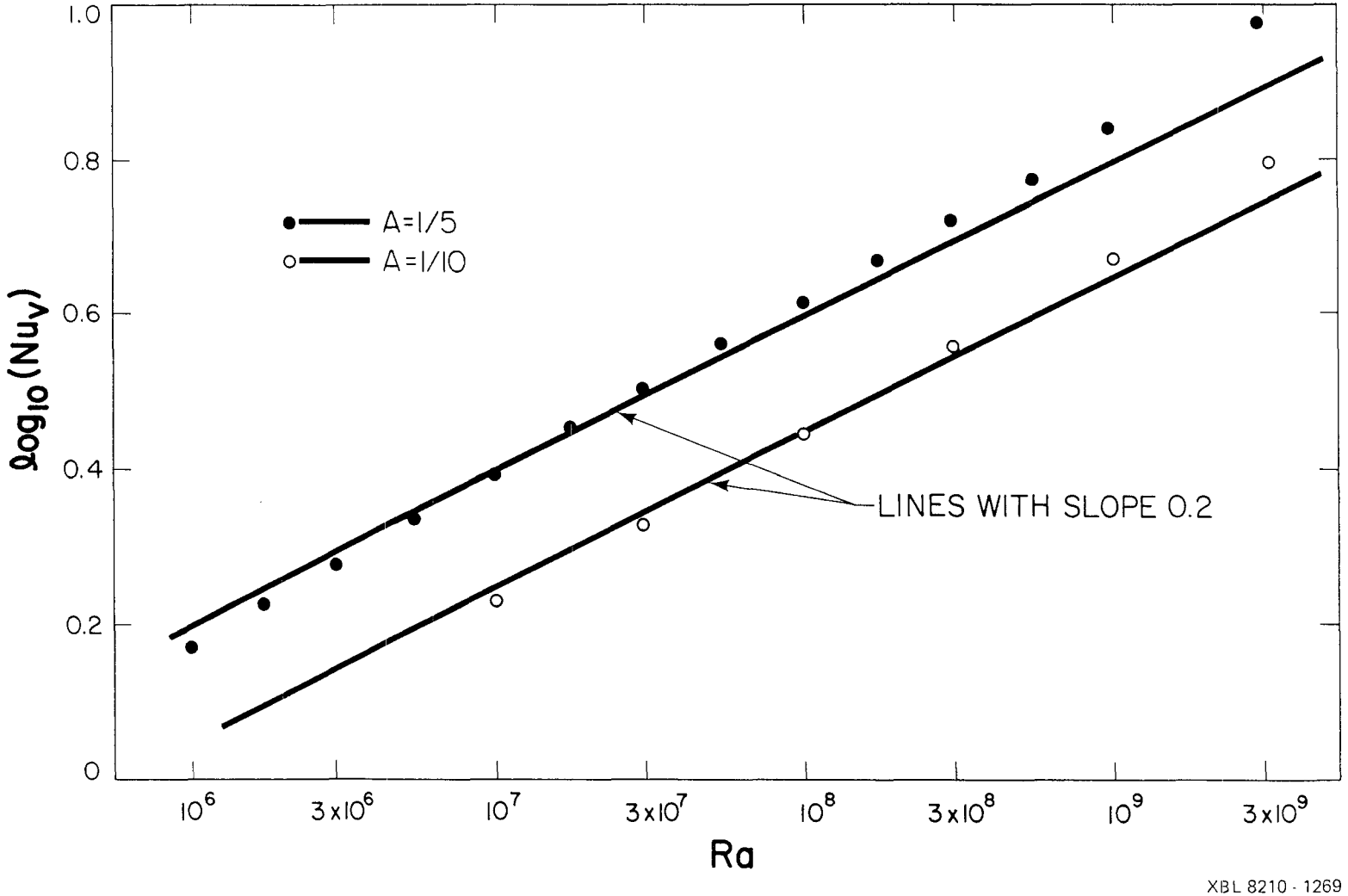

Figure 7. Nusselt Number on the Horizontal Walls as a Function of Rayleigh Number (Case I)

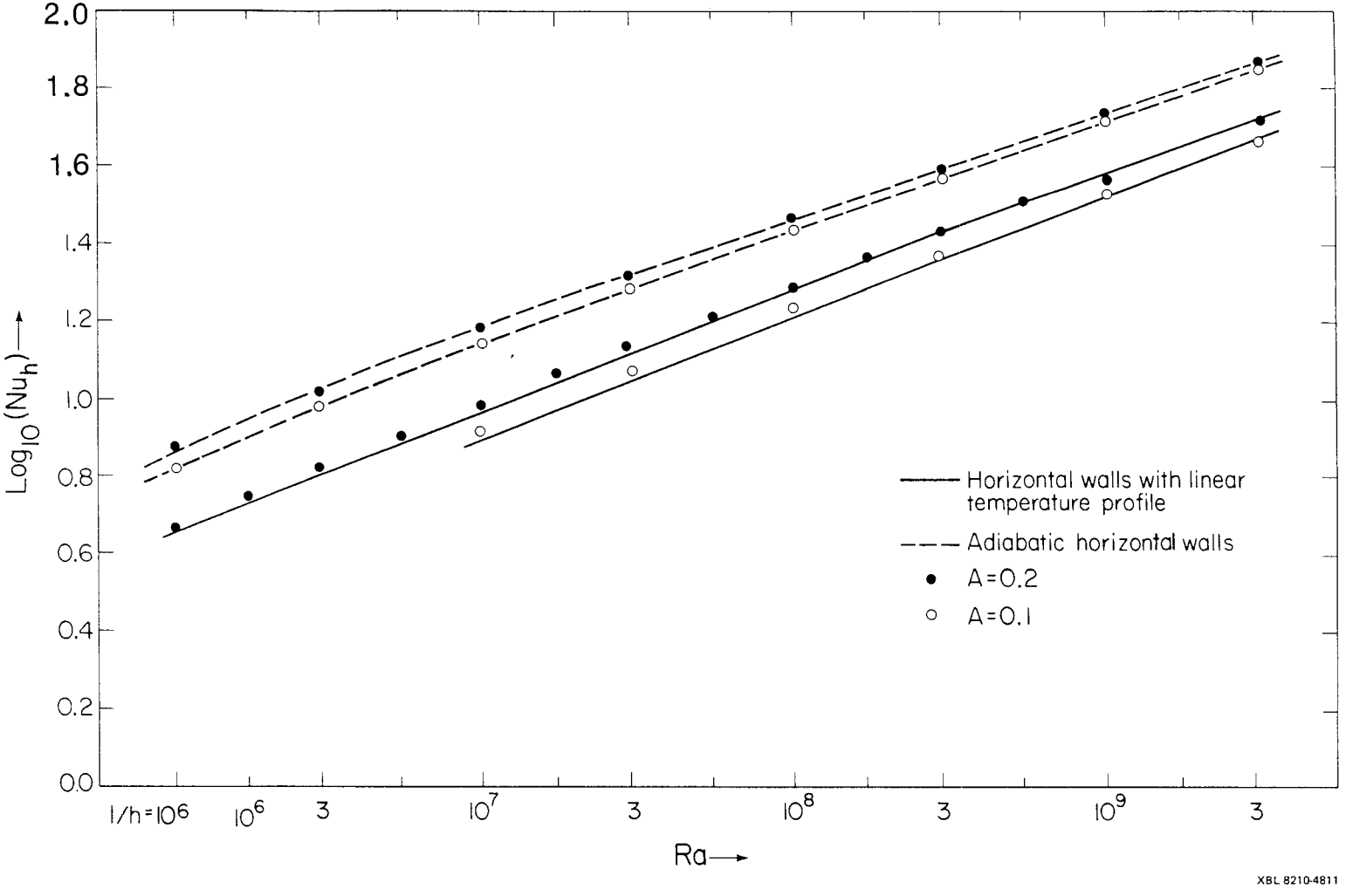

Figure 8. Nusselt Number on the Vertical (End) Walls as a Function of Rayleigh Number (Case I)

HORIZONTAL WALLS WITH SPECIFIED INTERACTION WITH ENVIRONMENT (CASE II)

In most laboratory studies seeking to simulate adiabatic horizontal walls for high Ra number convection in shallow enclosures, the experimenter must contend with some heat loss at the horizontal boundaries. Though a few experiments [21, 22] with very low losses have been reported, wall losses of about 25% are commonly reported [23]. Since, as shown below, even a small amount of heat transfer across the horizontal walls can qualitatively change the flow features, heat transfer results from such experiments must be interpreted with caution.

In order to gauge the impact of thermal interaction with the environment, numerical simulations were carried out at a fixed Ra number of 3.0×10^8 for two values of aspect ratio (0.1 and 0.2) with Pr = 1.0. The heat transfer coefficient [Eq. (4b)] between the horizontal wall and the external environment was varied over a wide range. The temperature of the external environment was taken to be the mean of the end wall temperatures.

The numerical simulations determined both the wall temperature profile and the wall heat flux profile consistent with Eq. (4b). At very small values of h, the horizontal walls are almost adiabatic since, from Eq. (4b), $(\partial\theta/\partial Y) \to 0$ as $h \to 0$.

Temperature profiles on the top horizontal wall for various values of h are displayed in Fig. 9 for A = 0.1. The corresponding velocity and temperature profiles along the vertical midsection are shown in Figs. 10a and 10b. The changes in the flow structure and the temperature profile are evident as the horizontal walls become more "lossy" (i.e., as h increases). As in Case I, the heat transfer to the horizontal walls produces both a temperature inversion in the horizontal boundary layers (which can result in flow inversion), and precooling/preheating of the flow approaching the cold/hot end walls (which results in a reduced Nu_h).

Figure 11 shows (Nu_v/A), the total heat transfer across the horizontal walls, as a function of Nu_h. Also shown is the heat transfer to the vertical walls expressed as a percentage of the heat transfer to the end walls $(100\ Nu_v/A\ Nu_h)$ against the horizontal heat transfer as a percentage of the heat transfer with adiabatic walls $(100\ Nu_h/Nu_h^*)$. The two curves for A = 0.1 and A = 0.2 fall quite close together. If one knows the ratio of horizontal to vertical heat transfer in an experiment (Case II), this figure can be used to obtain the approximate deviation of horizontal heat transfer from that which would be obtained if the walls were adiabatic. Data points with core flow reversals are indicated in the figure with solid symbols.

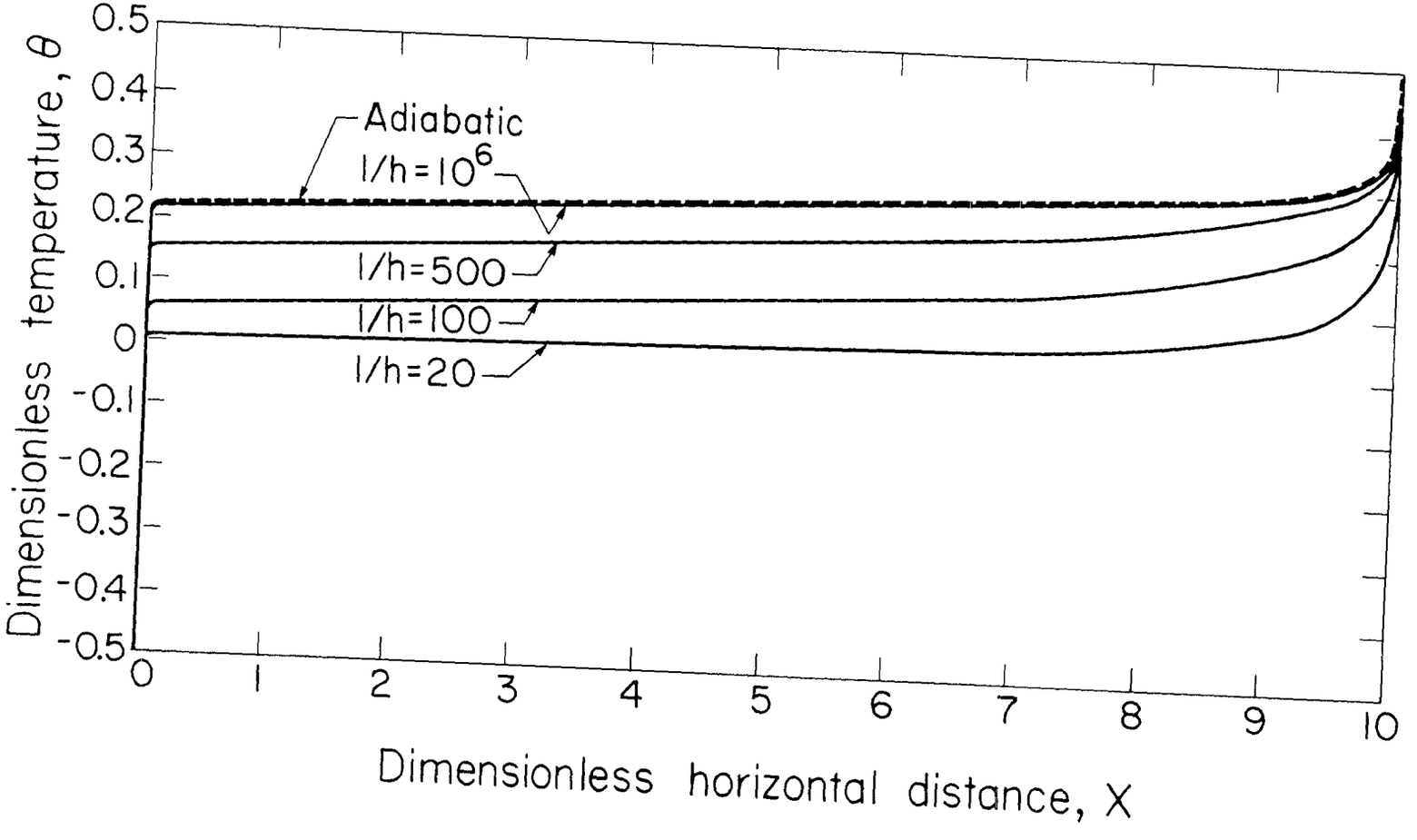

XBL 8210-4813

Figure 9. Temperature Profile on the Top Horizontal Wall as a Function of Distance (Case II)

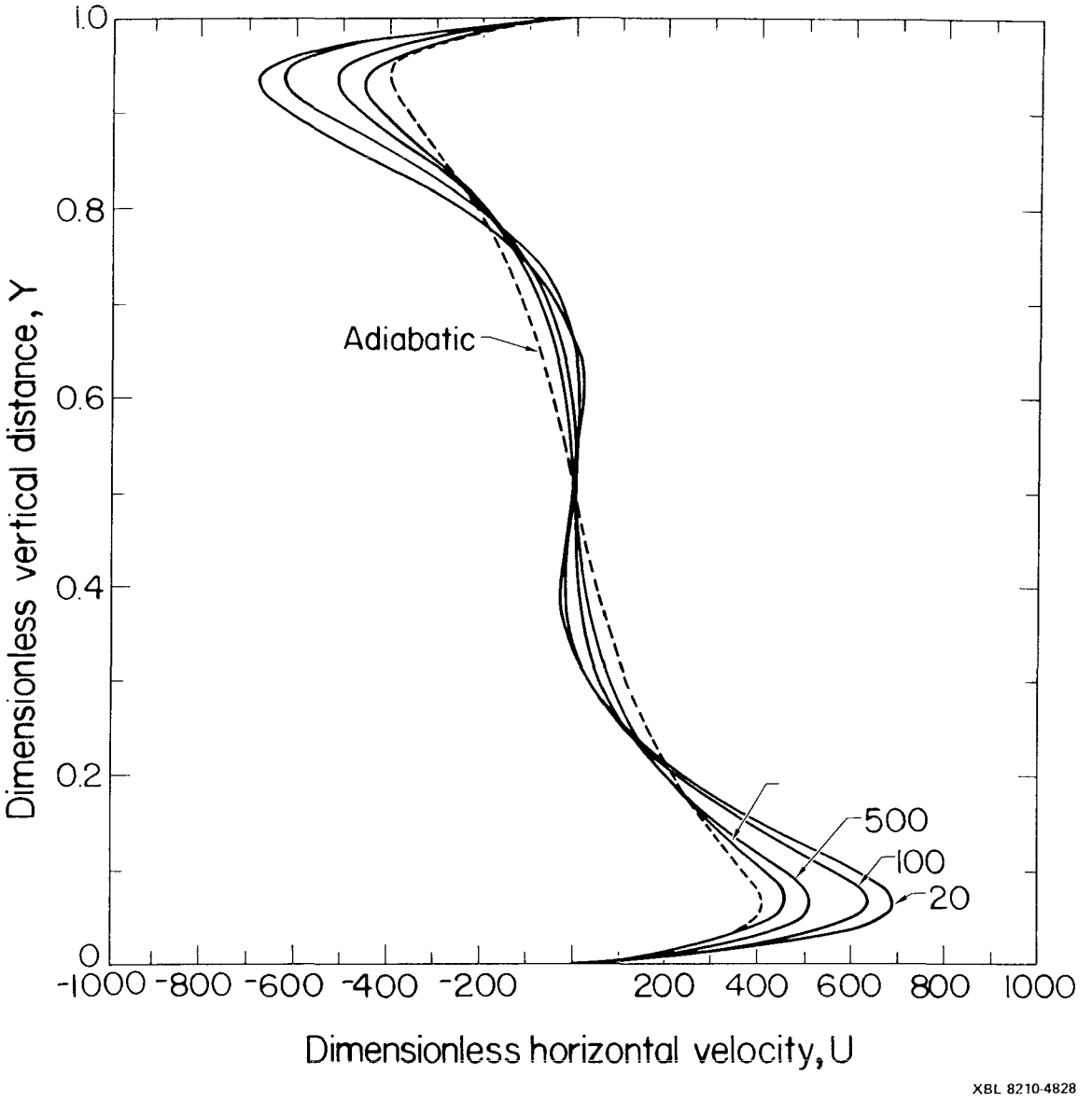

Figure 10a. Velocity Profile along Midsection (Case II)

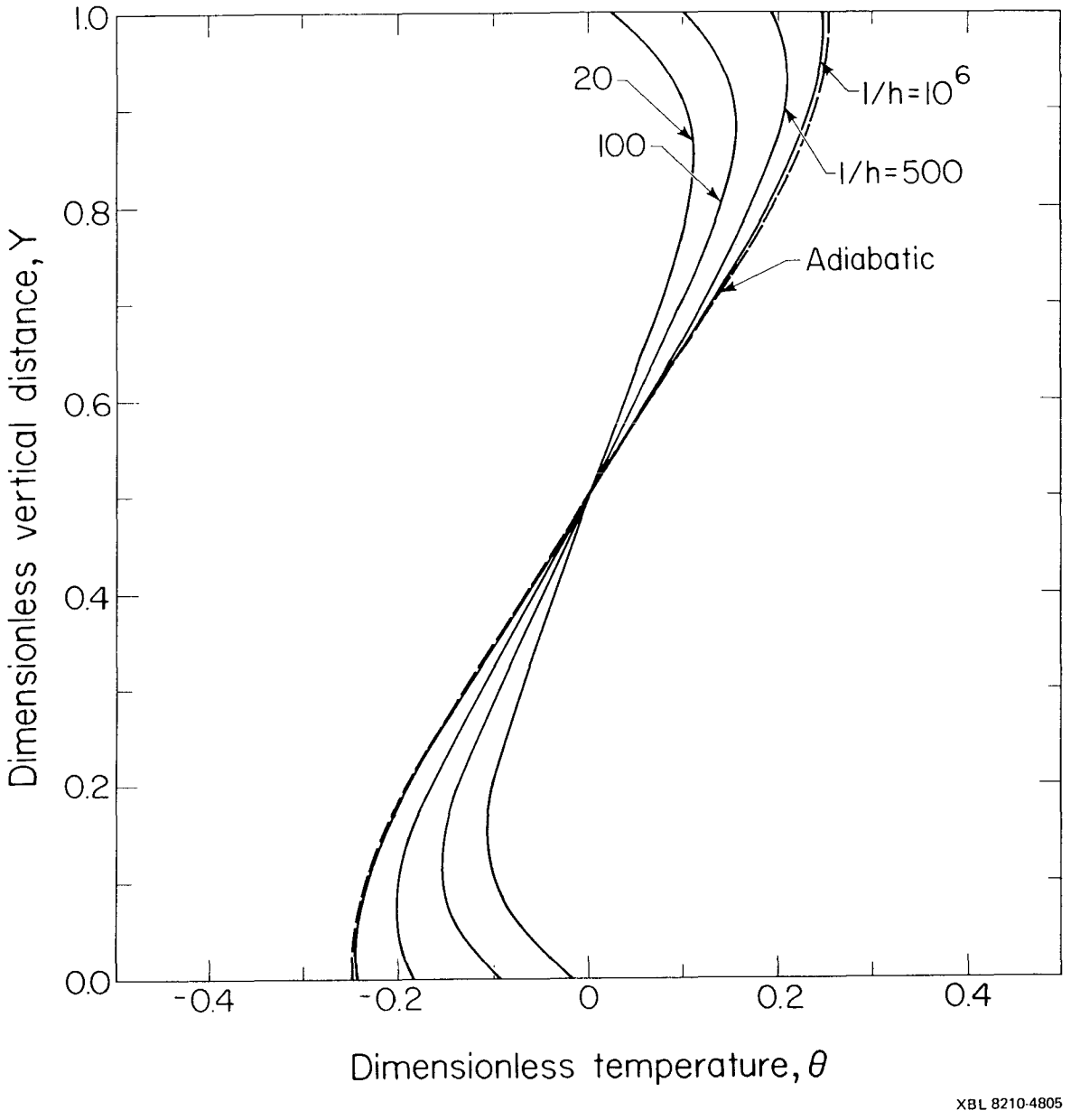

Figure 10b. Temperature Profile along Midsection (Case II)

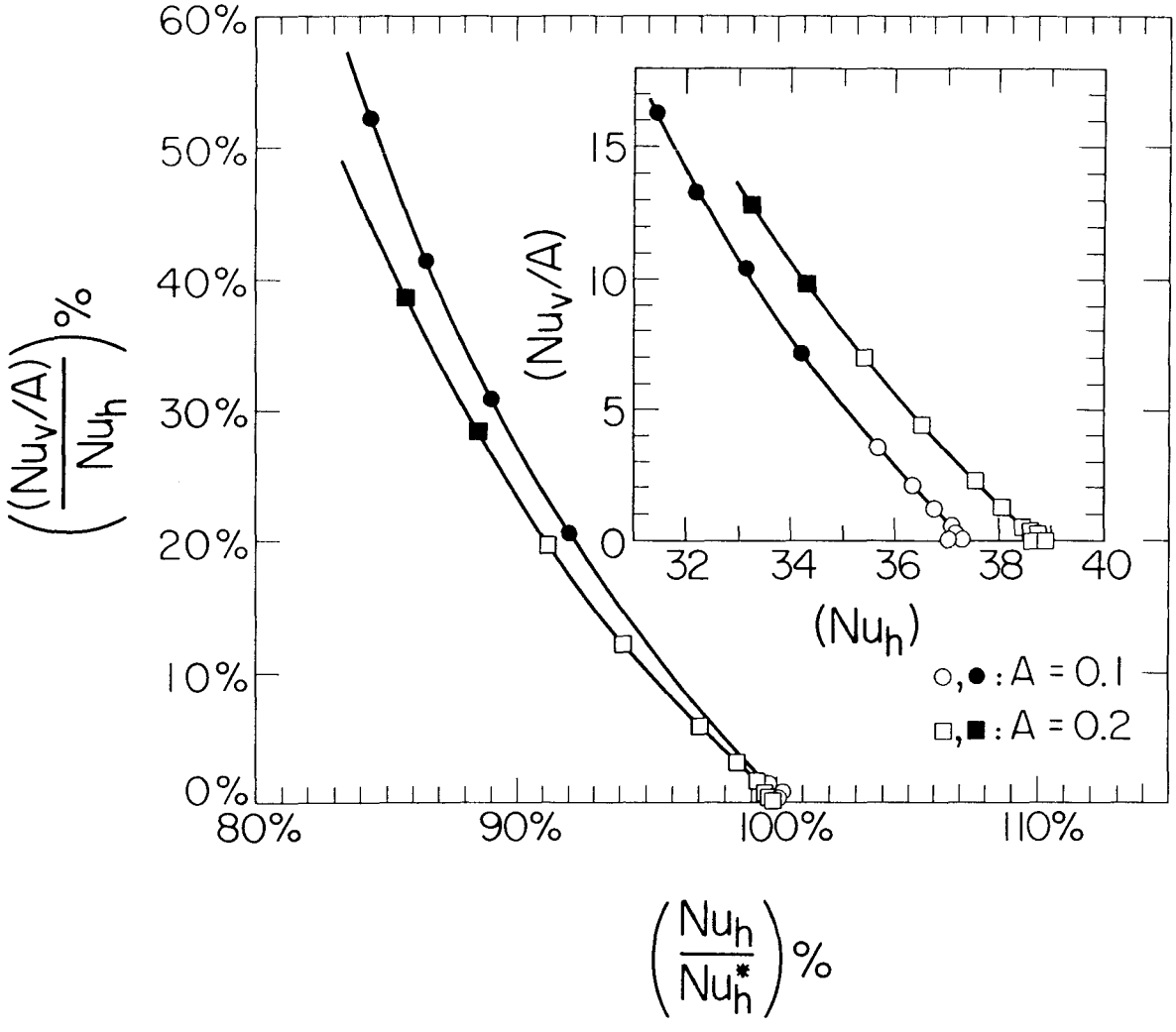

Figure 11. Ratio of Vertical to Horizontal Heat Transfer versus Horizontal Heat Transfer for Case II to Adiabatic Walls Case

ACKNOWLEDGMENTS

This work was funded by the Passive Research and Development Group, administered by Ron Kammerud and Wayne Place, of Lawrence Berkeley Laboratory. Their support and encouragement are greatly appreciated.

REFERENCES

1. S. Ostrach, "Natural Convection in Enclosures," Advances in Heat Transfer, 8 (1972).

2. I. Catton, "Natural Convection in Enclosures," Proceedings, Sixth Intl. Heat Transfer Conference, Toronto (1978).

3. A. Bejan, "Refrigeration for Rotating Superconducting Windings of Large AC Electric Machines," Cryogenics, 15, 3 (March 1976).

4. D.R. Smart, K.G.T. Hollands, and G.D. Raithby, "Free Convection Heat Transfer across Rectangular-Celled Diathermanous Honeycombs," J. Heat Transfer, 102, pp. 75-80 (Feb. 1980).

5. O.M. Phillips, "On Turbulent Convection Currents and the Circulation of the Red Sea," Deep Sea Research, 13, pp. 1149-1160 (1966).

6. H.B. Fischer, "Mass Transport Mechanism in Partially Stratified Estuaries," J. Fluid Mechanics, 65, part 2, pp. 671-687 (1972).

7. J. Imberger, "Natural Convection in Shallow Cavity with Differentially Heated End Walls, Part 3, Experimental Results," J. Fluid Mechanics, 65, pp. 247-260 (1974).

8. S. Ostrach, R.R. Loka, and A. Kumar, "Natural Convection in Low Aspect-Ratio Rectangular Enclosures," in Natural Convection in Enclosures, HTD Vol. 8, 19th National Heat Transfer Conference, Orlando, Florida, July 27-30 1980, sponsored by Heat Transfer Division of ASME.

9. G. Shiralkar, "Laminar Natural Convection in Rectangular Enclosures," Ph. D. Thesis, Department of Mechanical Engineering, University of California, Berkeley (1980).

10. A. Gadgil, "On Convective Heat Transfer in Building Energy Analysis," Ph.D. Thesis, Department of Physics, University of California, Berkeley (1979). Also issued as Lawrence Berkeley Laboratory Report LBL-10900 (1980).

11. F. Bauman, A. Gadgil, R. Kammerud, and R. Greif, "Buoyancy-Driven Convection in Rectangular Enclosures: Experimental Results and Numerical Calculations." Presented at the ASME Heat Transfer in Passive Solar Systems Conference, 27-30 July 1980, Orlando, FL, Paper No. 80-HT-66. Also published as Lawrence Berkeley Laboratory Report LBL-10257.

12 G. Shiralkar, A. Gadgil, and C.-L. Tien, "High Rayleigh Number Convection in Shallow Enclosures with Different End Temperatures," Int. J. Heat Mass Transfer, 24, 10, pp. 1621-1629 (1981).

13 J. Tichy and A. Gadgil, "High Rayleigh Number Laminar Convection in Low Aspect Ratio Enclosures with Adiabatic Horizontal Walls and Differentially Heated Vertical Walls," J. Heat Transfer, 104, pp. 103-110 (1982).

14. B.E. Boyak, and D.W. Kearney, "Heat Transfer by Laminar Natural Convection for Low Aspect Ratio Cavities," ASME paper No. 72-HT-52 (1972).

15. D.E. Cormack, L.G. Leal, and J.H. Seinfield, "Natural Convection in a Shallow Cavity with Differentially Heated End Walls, Part 2, Numerical Solutions," J. Fluid Mechanics, 65, pp. 231-246 (1974).

16. D.E. Cormack, L.G. Leal, and J. Imberger, "Natural Convection in a Shallow Cavity with Differentially Heated End Walls, Part 1, Asymptotic Theory," J. Fluid Mechanics, 65, pp. 209-229 (1974).

17. R.A. Wirtz, and W.-F. Tseng, "Natural Convection across Tilted, Rectangular Enclosures of Small Aspect Ratio," in ASME HTD-Vol. 8, Natural Convection in Enclosures, presented at the 19th National Heat Transfer Conference, Orlando, Florida, July 27-30 1980.

18. K. Klosse and P. Ullersma, "Convection in Vapour Transport Process," J. Crystal Growth, 18, North Holland Publishing Co. (1973).

19. A. Bejan and C.-L. Tien, "Laminar Natural Convection Heat Transfer in a Horizontal Cavity with Different End Temperatures," J. Heat Transfer, 100, pp. 641-647 (1978).

20. Al-Homoud and A. Bejan, "Experimental Study of High Rayleigh Number Convection in Shallow Horizontal Cavities with Different End Temperatures," Report CUMER-79-1, Department of Mechanical Engineering, University of Colorado, Boulder (1979).

21. F. Zirilli, "Physical Experiments in Free Convection in a Tilted Rectangular Enclosure of Aspect Ratio 0.1," Report No. MIE-053, Department of Mechanical and Industrial Engineering, Clarkson College, Potsdam, NY (May 1979).

22. J. Righi, "Physical Experiments on Free Convection in a Tilted Rectangular Enclosure of Aspect Ratio 0.2," Report No. MIE-062, Department of Mechanical and Industrial Engineering, Clarkson College, Potsdam, NY (August 1980).

23. D. Duxbury, "An Interferometric Study of Natural Convection in Enclosed Plane Air Layers with Complete and Partial Central Vertical Divisions," Ph.D. Thesis, University of Salford, United Kingdom (1979).

NOMENCLATURE

A = H/L, aspect ratio

g = acceleration due to gravity

Gr = $\beta\Delta T g H^3/\nu^2$, Grashof number

H = enclosure height

h = heat transfer coefficient on the outside of horizontal wall, Eq. (4b)

k = thermal conductivity

L = enclosure length

Nu_h = Nusselt number for horizontal heat transfer

Nu_v = Nusselt number for vertical heat transfer

Nu_h^* = Nusselt number for adiabatic horizontal walls case

Pr = ν/α, Prandtl number

Ra = $\beta\Delta T g H^3 Pr/\nu^2$, Rayleigh number

T = temperature

T_c = temperature of cold end wall

T_h = temperature of hot end wall

t = time

u = horizontal component of fluid velocity

$\vec{V}$ = fluid velocity vector

v = vertical component of fluid velocity

X = horizontal distance (dimensionless)

x = horizontal distance (dimensional)

Y = vertical distance (dimensionless)

y = vertical distance (dimensional)

Greek symbols

α = thermal diffusivity

β = coefficient of thermal expansion

Γ = velocity scale for horizontal boundary layer

δ = thickness of horizontal boundary layer

ΔT = $(T_h - T_c)$

θ = dimensionless temperature, $(T - (T_H+T_C)/2)/\Delta T$

θ_{env} = environment temperature (dimensionless)

ω = vorticity

ν = kinematic viscosity

$\vec{\nabla}$ = $(\partial/\partial X\ \hat{i} + \partial/\partial Y\hat{j})$, the gradient operator in X and Y

Δ^2 = $(\partial^2/\partial X^2 + \partial^2/\partial Y^2)$, the Laplacian operator in X and Y